An Event-Triggered Predictive Controller for Spacecraft Rendezvous Hovering Phases

Julio Sanchez, Christophe Louembet, Francisco Gavilan, Rafael Vazquez

An Event-Triggered Predictive Controller for Spacecraft Rendezvous Hovering Phases

Julio C. Sanchez * **Christophe Louembet** **
Francisco Gavilan * **Rafael Vazquez** *

* *Departamento de Ingeniería Aeroespacial, Universidad de Sevilla, Sevilla, Spain (e-mails: jsanchezm@us.es, fgavilan@us.es, rvazquez1@us.es).*
** *LAAS-CNRS, Université de Toulouse, CNRS, Toulouse, France (e-mail: louembet@laas.fr).*

Abstract: This work presents an event-triggered model predictive controller for spacecraft hovering phases. The target is flying in an elliptic orbit and is assumed to be inert whereas the chaser has impulsive thrusters. The main goal is to design a local controller based on event-triggering to keep the spacecraft within a hovering region while minimizing fuel consumption and avoiding unnecessary small amplitude firings. Using hybrid impulsive systems theory and reachability analysis, the invariance of the proposed method is studied. Simulation results are shown and discussed.

Keywords: Event-triggered control, Predictive control, Impulsive control, Spacecraft rendezvous

1. INTRODUCTION

In the context of spacecraft rendezvous, the hovering phase consists of a spacecraft maintaining its relative position within a bounded region with respect to a target spacecraft. This mission phase is especially relevant for orbit servicing operations with potential application to geostationary satellites servicing, see Barnhart et al. (2013), and spacecraft refuelling, see B. Reed et al. (2016).

In this paper, the target spacecraft is assumed to be inert and the chaser one is moved by means of chemical thrusters so that the control can be modelled by an impulsive signal. Some relevant works on impulsive control for rendezvous operations include Breger and How (2008), Di Cairano et al. (2012) and Yang and Cao (2015) whereas formation flying is addressed by Qi et al. (2012) and Gaias and D'Amico (2015).

The purpose of this study is to design an event-triggered predictive control strategy to maintain the spacecraft within the limits of a defined polytopic zone. Arantes Gilz et al. (2017) achieved station-keeping by controlling the spacecraft motion in the set of periodic trajectories included in the zone of interest. However, since the impulse sequence is computed at a fixed period, the obtained controls can be unnecessary or too small to be executed by the thrusters, especially if the system belongs or is close to the admissible set.

To overcome these drawbacks, an event-triggered model predictive controller is considered in this work for station-keeping. Event-based control is a control methodology where the commands are computed in an asynchronous way, reducing the communication needs between the sensors, the controller and the actuators in the control loop (see Aström (2008) for the basics). This methodology can be combined with feedback policies, see Wu et al. (2014) and references therein, and model-predictive schemes, see Pawlowski et al. (2015). In the context of spacecraft operations, event based controllers are recently attracting the attention of the attitude control community, see Wu et al. (2018) and Zhang et al. (2018), whereas some initial work for rendezvous hovering phases can be found in Louembet and Arantes Gilz (2018).

The main contribution of this paper is the development of a predictive controller using impulsive control in an asynchronous way. Its control objective is to locally stabilize the set of relative trajectories included in a given polytopic subset space. The scientific challenges arise from the linear time-varying dynamics and from the limited capability of the spacecraft thrusters which can only produce thrust of a minimum and maximum magnitude.

The present work extends and completes the initial communication by Louembet and Arantes Gilz (2018) in several directions. The definitions of the control laws are refined and explicitly detailed. The trigger laws have been redefined to ensure that all possible cases are covered. Additionally, the invariance of the proposed control approach is studied by using hybrid impulsive systems theory (Haddad et al. (2006)).

Note that the hybrid systems framework has been employed in the orbital rendezvous context recently. For instance, in the recent invited session "A Spacecraft Benchmark Problem for Analysis & Control of Hybrid Systems"

⋆ The authors gratefully acknowledge Universidad de Sevilla for funding part of this work through its V-PPI US.

that was presented at the 2016 IEEE Conference on Decision and Control. Moreover, in Brentari et al. (2018), a stability analysis of a given relative orbit has been done. The present paper focuses on the invariance of the set of periodic relative orbits that hover inside a given polytopic subspace. The proposed controller ensures local contractiveness.

The structure of this paper is as follows. Section 2 describes the relative motion model and the set of admissible orbits. Next, Section 3 presents both the control law and trigger law. Section 4 studies the invariance of the proposed controller. Section 5 shows results for cases of interest. Finally, Section 6 closes this paper with some additional considerations.

2. PROBLEM STATEMENT

In this section, first the relative motion model used to design the control law is explained. Then, the set of the constrained relative orbits for the hovering phase is presented, and a formal description based on envelope functions is provided.

2.1 Modelling the relative motion

The relative motion of the chaser spacecraft, denoted by S_f, is expressed with respect to the local frame attached to a passive target spacecraft whose position is denoted by S_l. The local frame $\{S_l, \boldsymbol{x}, \boldsymbol{y}, \boldsymbol{z}\}$, denoted Local Vertical/Local Horizontal (LVLH), moves around the inertial Earth-centered frame, $\{O, \boldsymbol{I}, \boldsymbol{J}, \boldsymbol{K}\}$, along the target spacecraft orbit. Note that $\boldsymbol{z}$ is the radial position (positive towards the centre of the Earth), $\boldsymbol{y}$ is the cross-track position (opposite to the orbit angular momentum) and $\boldsymbol{x}$ is the in-track position completing a right-handed system.

Under Keplerian assumptions, the relative motion between two spacecraft in the Earth gravitational field can be expressed by means of the Tschauner-Hempel equations, see Tschauner (1967). Considering that $\|\overrightarrow{OS_l}\| \gg \|\overrightarrow{S_l S_f}\|$, these equations can be linearized to obtain the following linear time-varying dynamics

$$\dot{X}(t) = A(t)X(t), \tag{1}$$

where the state vector X represents the relative position and velocity in the LVLH frame

$$X(t) = [x(t),\, y(t),\, z(t),\, \dot{x}(t),\, \dot{y}(t),\, \dot{z}(t)]^T.$$

In this work, the transition matrix of the dynamics (1) is exploited. To obtain this transition, a similarity transformation is applied

$$\tilde{X}(\nu) = T(\nu)X(t), \text{ with } T(\nu) = \begin{bmatrix} \rho\mathbb{I}_3 & 0_3 \\ \rho'\,\mathbb{I}_3 & \left(k^2\rho\right)^{-1}\mathbb{I}_3 \end{bmatrix}, \tag{2}$$

where $(\cdot)' = \frac{d(\cdot)}{d\nu}$, $k^2 = \sqrt{\frac{\mu}{a^3(1-e^2)^3}}$ and $\rho = 1 + e\cos\nu$. The transformation (2) is a change of the independent variable from time t to true anomaly of the target spacecraft, ν, which is the position of the target through its orbit. In this framework, the transition matrix can be computed (see Yamanaka and Ankersen (2002)) so that

$$\tilde{X}(\nu) = \Phi(\nu, \nu_0)\tilde{X}(\nu_0), \quad \nu_0 \le \nu. \tag{3}$$

In particular, the relative position can be explicitly expressed in a convenient manner as

$$\begin{aligned} \tilde{x}(\nu) &= d_1(1+\rho)s_\nu - d_2(1+\rho)c_\nu + d_3 + 3d_0 J(\nu)\rho^2, \\ \tilde{y}(\nu) &= d_4 c_\nu + d_5 s_\nu, \\ \tilde{z}(\nu) &= d_1\rho c_\nu + d_2\rho s_\nu - 3ed_0 J(\nu)s_\nu\rho + 2d_0, \end{aligned} \tag{4}$$

where e is the eccentricity of the target orbit and $J(\nu)$ is given by

$$J(\nu) := \int_{\nu_0}^{\nu} \frac{d\tau}{\rho(\tau)^2} = \sqrt{\frac{\mu}{a^3}}\frac{t - t_0}{(1-e^2)^{3/2}}. \tag{5}$$

As the orbital elements of a Keplerian orbit, the parameters d_0 to d_5 are integration constants that define the shape and position of the relative orbits, see (Deaconu, 2013, chap. 2). This fact makes the vector $D = [d_0,\ d_1,\ d_2,\ d_3,\ d_4,\ d_5]^T$ the relevant state when aiming to constrain relative orbits. Note that, a linear transformation exists between the relative state $\tilde{X}$ and the vector D

$$\tilde{X}(\nu) = F(\nu)D(\nu), \tag{6}$$

with

$$F(\nu) = \begin{bmatrix} 0 & s_\nu(1+\rho) & -c_\nu(1+\rho) & 1 & 0 & 0 \\ 0 & 0 & 0 & 0 & c_\nu & s_\nu \\ 2 & c_\nu\rho & s_\nu\rho & 0 & 0 & 0 \\ 3 & 2c_\nu\rho - e & 2s_\nu\rho & 0 & 0 & 0 \\ 0 & 0 & 0 & 0 & -s_\nu & c_\nu \\ -\dfrac{3es_\nu}{\rho} & -s_\nu(1+\rho) & 2ec_\nu^2 - e + c_\nu & 0 & 0 & 0 \end{bmatrix}.$$

Since $\det F = 1 - e^2 \neq 0,\ \forall e \in [0, 1)$, it represents a similarity transformation and D is a proper state vector with its own dynamics,

$$D'(\nu) = \underbrace{\begin{bmatrix} 0 & 0\,0\,0\,0\,0 \\ 0 & 0\,0\,0\,0\,0 \\ -\frac{3e}{\rho^2} & 0\,0\,0\,0\,0 \\ \frac{3}{\rho^2} & 0\,0\,0\,0\,0 \\ 0 & 0\,0\,0\,0\,0 \\ 0 & 0\,0\,0\,0\,0 \end{bmatrix}}_{A_D(\nu)} D(\nu), \tag{7}$$

and its own transition matrix,

$$D(\nu) = \underbrace{\begin{bmatrix} 1 & 0\,0\,0\,0\,0 \\ 0 & 1\,0\,0\,0\,0 \\ -3eJ(\nu) & 0\,1\,0\,0\,0 \\ 3J(\nu) & 0\,0\,1\,0\,0 \\ 0 & 0\,0\,0\,1\,0 \\ 0 & 0\,0\,0\,0\,1 \end{bmatrix}}_{\Phi_D(\nu,\nu_0)} D(\nu_0). \tag{8}$$

Typically, for space hovering operations, the chaser spacecraft is controlled by chemical engines that provide a high level of thrust during a short time with respect to the target orbit period. This fact leads to extremely fast changes of velocities that can be modelled as impulses

$$X^+(t) = X(t) + B\Delta V(t), \text{ with } B = [0_3, \mathbb{I}_3]^T, \tag{9}$$

where 0_3 is the square null matrix and $\mathbb{I}_3$ is the identity matrix, both of dimension 3. Applying the changes of variable (2) and (6), an impulse at instant ν produces a jump in the D state as

$$D^+(\nu) = D(\nu) + B_D(\nu)\Delta V(\nu), \tag{10}$$

with

$$B_D(\nu) = F^{-1}(\nu)T(\nu)B, \tag{11}$$

and hence

$$B_D(\nu) = \frac{1}{k^2(e^2-1)\rho}\begin{bmatrix} \rho^2 & 0 & -es_\nu\rho \\ -2c_\nu - e(1+c_\nu^2) & 0 & s_\nu\rho \\ -s_\nu(2+ec_\nu) & 0 & 2e - c_\nu\rho \\ es_\nu(2+ec_\nu) & 0 & ec_\nu\rho - 2 \\ 0 & -(e^2-1)s_\nu & 0 \\ 0 & (e^2-1)c_\nu & 0 \end{bmatrix}.$$

Equation (10) shows that a given impulsive control, ΔV, will have a different influence depending on the instant of application due to the time dependence of the input matrix B_D. Additionally, the thrust magnitude along each axis has to comply with the following conditions on deadzone and saturation

$$\underline{\Delta V} \leq |\Delta V| \leq \overline{\Delta V}. \tag{12}$$

The previous facts have to be accounted for in order to design the event-triggered controller.

2.2 Semi-algebraic description of the constrained orbits set

The goal of our predictive controller is to maintain the spacecraft hovering in a predefined polytopic subset of the relative position space. Thereafter, a cuboid is considered without loss of generality:

$$\underline{x} \leq x(t) \leq \overline{x},\ \underline{y} \leq y(t) \leq \overline{y},\ \underline{z} \leq z(t) \leq \overline{z}\,,\ \forall t \geq t_0. \tag{13}$$

The most economic way to hover in a given zone, is that the chaser evolves on periodic orbits. In the relative motion framework, a relative orbit is periodic if and only if its parameter D satisfy the periodicity condition $d_0 = 0$. This condition can be derived from (4) by noting that the only non periodic term $J(\nu)$ is weighted by the state d_0. Inserting the changes of variables (2) and (6) into (13) and considering the periodicity condition, the admissible set S_D^p can be formally defined as

$$S_D^p := \left\{ D \in \mathbb{R}^6 \;\middle|\; d_0 = 0,\ \begin{matrix} \underline{x} \leq F_x(\nu)D \leq \overline{x} \\ \underline{y} \leq F_y(\nu)D \leq \overline{y} \\ \underline{z} \leq F_z(\nu)D \leq \overline{z} \end{matrix},\forall \nu \right\}, \tag{14}$$

where F_x, F_y and F_z are, respectively the first three rows of F divided by ρ. The set S_D^p is described by linear but time-varying conditions on the state D.

In Arantes Gilz et al. (2017), an implicitization method is developed to obtain a semi-algebraic description of the admissible set:

$$S_D^p = \{D \in \mathbb{R}^6 \mid d_0 = 0 \mid g_w(D) \leq 0, \quad \forall w \in \{\overline{x}, \underline{x}, \overline{y}, \underline{y}, \overline{z}, \underline{z}\}\}. \tag{15}$$

where the functions $g_w(D)$ are given by

$$g_{\underline{x}}(d_1, d_2, d_3) = r_{\underline{x}}(d_1, d_2, e, \underline{x}) - d_3, \tag{16}$$
$$g_{\overline{x}}(d_1, d_2, d_3) = d_3 - r_{\overline{x}}(d_1, d_2, e, \overline{x}), \tag{17}$$
$$g_{\underline{y}}(d_4, d_5) = (d_4 - e\underline{y})^2 + d_5^2 - \underline{y}^2, \tag{18}$$
$$g_{\overline{y}}(d_4, d_5) = (d_4 - e\overline{y})^2 + d_5^2 - \overline{y}^2, \tag{19}$$
$$g_{\underline{z}}(d_1, d_2) = d_1^2 + d_2^2 - \underline{z}^2, \tag{20}$$
$$g_{\overline{z}}(d_1, d_2) = d_1^2 + d_2^2 - \overline{z}^2, \tag{21}$$

where $r_{\underline{x}}$ and $r_{\overline{x}}$ denote the largest and smallest real roots of the following polynomials in d_3

$$\hat{g}_{\underline{x}}(d_1, d_2, d_3) = \sum_{i=0}^{4} \theta_{\underline{x},i}(d_1, d_2) d_3^i, \tag{22}$$

$$\hat{g}_{\overline{x}}(d_1, d_2, d_3) = \sum_{i=0}^{4} \theta_{\overline{x},i}(d_1, d_2) d_3^i. \tag{23}$$

The interested reader is referred to Arantes Gilz et al. (2017) for explicit details.

3. EVENT-BASED ALGORITHM

In this section, the control and trigger laws that constitute the event-triggered controller are designed. One must notice that the trigger law determines when to apply a suitable control law.

3.1 Control law

By inspecting the transition matrix (8) and the spatial constraints (14) it can be seen that the in-plane and out-of-plane control problems are decoupled and thus can be treated separately.

In-plane control Let us define the in-plane motion by the state subset $D_{xz}=[d_0, d_1, d_2, d_3]^T$. As stated earlier, periodicity is a desirable property to hover over a specified region, therefore, the in-plane control strategy aims to steer the system to a periodic orbit with one impulsive control. Hence, the in-plane state after an in-plane impulse $\Delta V_{xz}=[\Delta V_x, \Delta V_z]^T$ is given by $D_{xz}^+(\nu) = D_{xz}(\nu) + B_{D,xz}(\nu)\Delta V_{xz}(\nu)$ where $B_{D,xz}\in\mathbb{R}^{4\times 2}$ is composed by the in-plane terms of B_D. In particular, the state d_0 is controlled such that

$$d_0^+(\nu) = d_0(\nu) + B_{d_0,xz}(\nu)\Delta V_{xz}(\nu) = 0, \tag{24}$$

where $B_{d_i,xz}$ with i=0...3 is the (i+1)th row of $B_{D,xz}$. A control satisfying (24) is written as

$$\Delta V_{xz}(\nu) = \lambda_{xz} B_{d_0,xz}^{\perp}(\nu) + \Delta V_{xz}^0(\nu), \tag{25}$$

where $\lambda_{xz}\in\mathbb{R}$, $B_{d_0,xz}^{\perp}\in\mathbb{R}^2$ describes the kernel space of $B_{d_0,xz}$ and $\Delta V_{xz}^0\in\mathbb{R}^2$ is a particular solution of (24). With this periodicity pursuing strategy, the effect of a control impulse on the current state D is described by

$$\begin{aligned} D_{xz}^+(\nu, \lambda_{xz}) =& D_{xz}(\nu) + \\ & B_{D,xz}(\nu)(\lambda_{xz} B_{d_0,xz}^{\perp}(\nu) + \Delta V_{xz}^0(\nu)), \end{aligned} \tag{26}$$

To maintain the state D_{xz} in the admissible set $S_{D_{xz}}^p$ at time ν, the following program is solved

$$\begin{aligned} &\min_{\lambda_{xz}} \|\Delta V_{xz}(\nu, \lambda_{xz})\|_1, \\ &\text{s.t.} \begin{cases} D_{xz}^+(\nu) \in S_{D_{xz}}^p, \\ \lambda_{xz} \in I_{sat,xz}(\nu), \end{cases} \end{aligned} \tag{Psat,in}$$

where $I_{sat,xz}$ describes the input saturation and deadzone condition as a function of λ_{xz} and ν such that

$$\begin{aligned} I_{sat,xz} = \{&\lambda_{xz} \in \mathbb{R} \text{ s.t.} \\ &\underline{\Delta V} \leq |\lambda_{xz} B_{d_{0,xz}}^{\perp}(\nu) + \Delta V_{xz}^0(\nu)| \leq \overline{\Delta V}\} = \\ &[\overline{l^-},\ \underline{l^-}] \cup [\underline{l^+},\ \overline{l^+}], \end{aligned} \tag{27}$$

where $\overline{l^-}=(B_{d_{0,xz}^{\perp}})^+(-\overline{\Delta V} - \Delta V_{xz}^0)$, $\underline{l^-}=(B_{d_{0,xz}^{\perp}})^+(-\underline{\Delta V} - \Delta V_{xz}^0)$, $\overline{l^+}=(B_{d_{0,xz}^{\perp}})^+(\overline{\Delta V} - \Delta V_{xz}^0)$ and $\underline{l^+}=(B_{d_{0,xz}^{\perp}})^+(\underline{\Delta V} - \Delta V_{xz}^0)$.

Out-of-plane control The out-of-plane motion, represented by $D_y = [d_4, d_5]^T$, is naturally periodic and any out-of-plane control $\Delta V_y{=}\lambda_y$ produces a periodic orbit. Consequently, the effect of an out-of-plane impulse on the current state D is given by

$$D_y^+(\nu, \lambda_y) = D_y(\nu) + \lambda_y B_{D,y}(\nu), \tag{28}$$

and to steer the state D_y to the admissible set $S^p_{D_y}$ at time ν, the following program is solved

$$\min_{\lambda_y} \|\Delta V_y(\nu, \lambda_y)\|_1, \quad \text{s.t. } \begin{cases} D_y^+(\nu) \in S^p_{D_y}, \\ \lambda_y \in I_{sat,y}, \end{cases} \tag{Psat,out}$$

where $I_{sat,y}$ describes the input saturation and deadzone conditions such that

$$I_{sat,y} = [-\overline{\Delta V},\ \underline{\Delta V}] \cup [-\underline{\Delta V},\ \overline{\Delta V}]. \tag{29}$$

Note that $I_{sat,y}$ does not depend on ν.

3.2 Instantaneous reachability conditions

To set the trigger rules, instantaneous S^p_D reachability conditions needs to be set at a given time instant ν. Note that, for the sake of the clarity of the notation, the time dependence is omitted in this section. First, let the set Δ^+ be the reachable set of D^+ from D with one control. Δ^+ is a two-dimensional plane on the D space, defined by the lines Δ^+_{xz} and Δ^+_y

$$\Delta^+_{xz} = \{D^+_{xz} \in \mathbb{R}^4 \text{ s.t. } (26), \lambda_{xz} \in \mathbb{R}\}, \tag{30}$$

$$\Delta^+_y = \{D^+_y \in \mathbb{R}^2 \text{ s.t. } (28), \lambda_y \in \mathbb{R}\}. \tag{31}$$

A necessary condition for the admissible set S^p_D to be reachable is that the following sets Λ^+_{xz} and Λ^+_y are non-empty:

$$\Lambda^+_{xz} = [\underline{l_{xz}}, \overline{l_{xz}}], \tag{32}$$

$$\Lambda^+_y = [\underline{l_y}, \overline{l_y}]. \tag{33}$$

The intervals $[\underline{l_{xz}}, \overline{l_{xz}}]$ and $[\underline{l_y}, \overline{l_y}]$ are computed such that at a given fixed instant ν

$$\forall \lambda_{xz} \in [\underline{l_{xz}}, \overline{l_{xz}}] : \{g_{\overline{x}}(\lambda_{xz}) \le 0,\ g_{\underline{x}}(\lambda_{xz}) \le 0,\ g_{\overline{z}}(\lambda_{xz}) \le 0,\ g_{\underline{z}}(\lambda_{xz}) \le 0\}, \tag{34}$$

$$\forall \lambda_y \in [\underline{l_y}, \overline{l_y}] : \{g_{\overline{y}}(\lambda_y) \le 0,\ g_{\underline{y}}(\lambda_y) \le 0\}. \tag{35}$$

Note that the univariate polynomials $g_w(\lambda_{xz}, \lambda_y)$ are obtained by introducing the expressions (26) and (28), in λ_{xz} and λ_y respectively, in (22)-(23), (20)-(21) and (18)-(19). Moreover, accounting for the saturation and deadzone conditions (12), S^p_D is reachable if and only if the sets $\Lambda^+_{sat,xz}$ and $\Lambda^+_{sat,y}$ are non-empty:

$$\Lambda^+_{sat,xz} = [\underline{l_{xz}}, \overline{l_{xz}}] \cap I_{sat,xz} \neq \emptyset, \tag{36}$$

$$\Lambda^+_{sat,y} = [\underline{l_y}, \overline{l_y}] \cap I_{sat,y} \neq \emptyset. \tag{37}$$

Note that the sets of reachable admissible states, $\Delta^+_{sat,xz}$ and $\Delta^+_{sat,y}$, are given by

$$\Delta^+_{xz} = \{D^+_{xz} \in \mathbb{R}^4 \text{ s.t. } (26), \lambda_{xz} \in \Lambda^+_{sat,xz}\}, \tag{38}$$

$$\Delta^+_y = \{D^+_y \in \mathbb{R}^2 \text{ s.t. } (28), \lambda_y \in \Lambda^+_{sat,y}\}. \tag{39}$$

Let us define the following variables that measure the length of the intervals $\Lambda^+_{sat,xz}$ and $\Lambda^+_{sat,y}$ and its time derivative

$$L_{xz} = \text{len}(\Lambda^+_{sat,xz}), \quad L_y = \text{len}(\Lambda^+_{sat,y}), \tag{40}$$

$$L_{\nu,xz} = \frac{dL_{xz}}{d\nu}, \quad L_{\nu,y} = \frac{dL_y}{d\nu}. \tag{41}$$

These variables will be used as an oracle for the S^p_D instantaneous reachability in the triggering strategy section.

3.3 Reachability conditions over one period

In the previous section, instantaneous reachability conditions on S^p_D are set for a given instant ν. This section establishes that S^p_D is reachable over the next 2π-period (a complete revolution) assuming that the current state D is an equilibrium point ($d_0 = 0$). Recalling that the control matrix B_D is 2π-periodic, computing the reachable set from a given state over a 2π-period can be done through implicitization techniques. In order to simplify the following notation, we introduce the state increment

$$\Delta D(\nu) = D^+(\nu) - D(\nu) = B_D(\nu)\Delta V(\nu) = [\Delta d_0,\ \Delta d_1,\ \Delta d_2,\ \Delta d_3,\ \Delta d_4,\ \Delta d_5]^T. \tag{42}$$

Considering the out-of-plane motion, the state increment is represented by $\Delta D_y = [\Delta d_4(\nu),\ \Delta d_5(\nu)]$. The incremental reachable set over an orbital period depends on the control effort λ_y and is implicitly described by

$$f_y(\Delta D, \lambda_y) = \frac{\Delta d_4^2}{\left(\frac{\lambda_y}{k^2\sqrt{1-e^2}}\right)^2} + \frac{\left(\Delta d_5 + \frac{e\lambda_y}{k^2(1-e^2)}\right)^2}{\left(\frac{\lambda_y}{k^2(1-e^2)}\right)^2} - 1 = 0. \tag{43}$$

Note that (43) is an ellipse in the Δd_4-Δd_5 plane. Its semi-axes and center are both affected by the control parameter, λ_y. Hence, for given deadzone and saturation conditions $\lambda_y \in I_{sat}$, the incremental reachable set is described by

$$\mathcal{D}_{f_y} = \mathcal{D}_{f_y,-} \cup \mathcal{D}_{f_y,+}, \tag{44}$$

where

$$\mathcal{D}_{f_y,-} := \{\Delta D \in \mathbb{R}^6 : f_y(\Delta D, -\underline{\Delta V}) \ge 0,\ f_y(\Delta D, -\overline{\Delta V}) \le 0\}. \tag{45}$$

$$\mathcal{D}_{f_y,+} := \{\Delta D \in \mathbb{R}^6 : f_y(\Delta D, \underline{\Delta V}) \ge 0,\ f_y(\Delta D, \overline{\Delta V}) \le 0\}. \tag{46}$$

By computing the Minkowski sum of S^p_D, the admissible set, with the incremental reachable set (44),

$$\mathcal{D}_{c,\text{out}} := S^p_{D_y} \oplus \mathcal{D}_{f_y}, \tag{47}$$

one obtains a subset of the state from where S^p_D can be reached by means of impulsive control (see Fig.1). Regarding the in-plane motion, both in-track (x) and radial (z) constraints have to be addressed. The in-plane control action, (26), can be implicitized for $d_0{\approx}0$ using a Gröbner basis as in Fix et al. (1996)

$$4\Delta d_1^2 + (-e^2+4)\Delta d_2^2 + 2e\Delta d_2\Delta d_3 - \Delta d_3^2 = 0. \tag{48}$$

Note that (48) is the equation of a cone representing the unconstrained in-plane incremental reachable set over a target orbital period. However, the implicitization is only valid if all the instants over a target orbital period are allowed which is not the case due to (27). Therefore, the in-plane attainable set is studied by numerical means.

The numerical method is designed by defining a volume Ω in the $d_1d_2d_3$ space embedding $S^p_{D_{xz}}$. For discrete points, $D_j{\in}\Omega$, of the previously defined volume, intersections

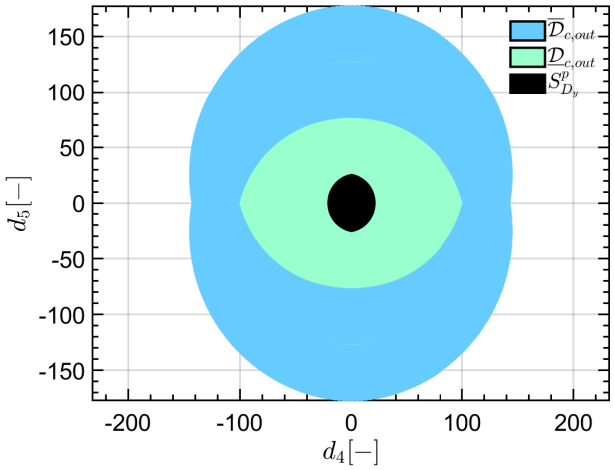

Fig. 1. $\underline{\mathcal{D}}_{c,\text{out}}$ and $\overline{\mathcal{D}}_{c,\text{out}}$ for Table 1 parameters.

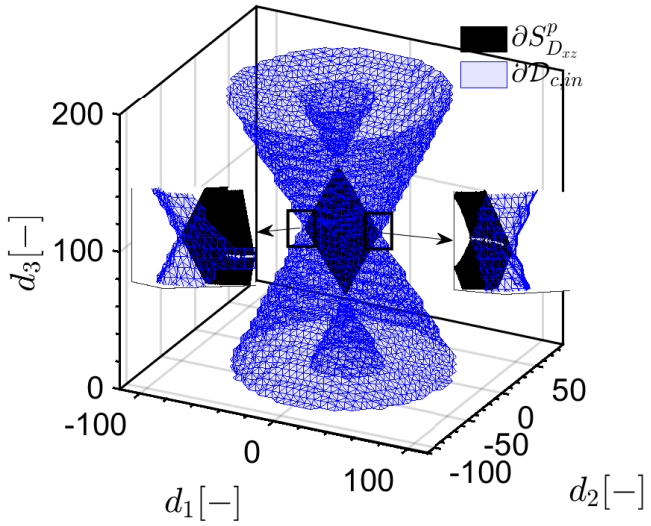

Fig. 2. $\partial\mathcal{D}_{c,in}$ for Table 1 parameters.

between the admissible set and the constrained reachable set can be computed $\Delta^+_{sat,xz}(D_j,\nu_i)$ where $\nu_i\in[0,2\pi]$ are discrete true anomalies. Then, the value $L_{xz,2\pi}(D_j) = \sum_{i=1}^{N_\nu} \text{len}(\Lambda^+_{sat,xz}(D_j,\nu_i))$ is estimated. If $L_{xz,2\pi}(D_j)\neq 0$, then exists an instant ν_i for which S^p_D is reachable from D_j so that $D_j \in \mathcal{D}_{c,\text{in}}$. $\partial\mathcal{D}_{c,\text{in}}$, the boundary of $\mathcal{D}_{c,\text{in}}$ can be numerically interpolated and is shown in Fig. 2. For the previous figure, 64000 points within a cube of 200×200×200 dimensions centered at $[0,0,100]^T$ in the $d_1d_2d_3$ space defines Ω. For each D_j, it has been assumed $d_{0,j}$=0.

In conclusion, S^p_D is reachable over a 2π-period if and only if $D \in \mathcal{D}_c = \mathcal{D}_{c,\text{in}} \times \mathcal{D}_{c,\text{out}}$.

3.4 Trigger law

The trigger law is designed to achieve a threefold objective. Firstly the programs (Psat,in) and (Psat,out) have to be feasible when executed. Secondly, unnecessary controls must be avoided. Finally, Zeno phenomena should be ensured to not occur.

Using the definitions from previous section, the triggering decision is made according to Algorithm 1, which sends a trigger each time the spacecraft leaves the admissible set S^p_D based on (15). Note that Algorithm 2 chooses the suitable control program when a trigger signal is raised and is valid for both in-plane and out-of-plane control.

Algorithm 1 (Trigger rules)

Input: ν, D
Output: control decision
  if $D(\nu) \in S^p_D$ **then**
    Wait.
  else
    Call algorithm 2
  end if

Algorithm 2 (Strategy to reach the admissible set S^p_D)

Input: ν, D
Output: control decision
  if $D(\nu)\notin S^p_{D_{xz}}$ **then**
    if $L_{xz}(\nu)<\delta$ & $L_{\nu,xz}(\nu)<0$ **then**
      Solve (Psat,in) and apply ΔV_{xz}.
    else if $L_{xz}(\nu)=0$ **then**
      if $D\in\mathcal{D}_c$ **then**
        Wait until ν_p such that $L_{xz}(\nu_p)\neq 0$,
      else
        Apply the controller of Arantes Gilz et al. (2018)
      end if
    else
      Wait
    end if
  end if
  if $D(\nu)\notin S^p_{D_y}$ **then**
    if $L_y(\nu)<\delta$ & $L_{\nu,y}(\nu)<0$ **then**
      Solve (Psat,out) and apply ΔV_y.
    else if $L_y(\nu)=0$ **then**
      if $D\in\mathcal{D}_c$ **then**
        Wait until ν_p such that $L_y(\nu_p)\neq 0$,
      else
        Apply the controller of Arantes Gilz et al. (2018)
      end if
    else
      Wait
    end if
  end if

To summarize, the strategy to reach S^p_D consists in first computing $\Lambda^+_{sat}(\nu)$. An impulse control is triggered if $L(\nu)$ is below a given threshold, δ, and is contracting $L_\nu(\nu)<0$. Note that the previous variables are computed for the corresponding in-plane or out-of-plane motion. Otherwise, the trigger law awaits for the length to diminish in order to avoid unnecessary impulses accordingly to event-triggered control philosophy. In the case where the admissible set is not reachable at the current instant but is expected to be in the next 2π period ($D\in\mathcal{D}_c$), the controller awaits until S^p_D becomes reachable again to apply a control action. If it is not the case, the 3-impulsive approach of Arantes Gilz et al. (2018), assuring global convergence to S^p_D, can be employed.
Note that Zeno-type behaviours are avoided by the presence of deadzone conditions in (27) and (29).

4. INVARIANCE OF THE SINGLE-IMPULSE APPROACH

In this section, the invariance of the proposed event-based predictive controller is studied. Firstly, some fundamental results of invariance for hybrid impulsive systems are summarized. Then the out-of-plane and in-plane invariance are analyzed.

4.1 Invariance for hybrid impulsive systems

The relative motion between target and chaser is equivalent to an hybrid impulsive system composed of the continuous dynamics of (7) and the resets of (10). Therefore, the main results of Haddad et al. (2006) regarding invariance principles for hybrid impulsive systems apply. Consider the following dynamical system $\mathcal{G}$

$$\begin{array}{ll} \dot{x}(t) & = f_c(x(t)),\ x(0)=x_0,\ x_0\in\mathcal{D},\quad x(t)\notin\mathcal{Z},\\ \Delta x(t) & = f_d(x(t)), \qquad\qquad\qquad\quad x(t)\in\mathcal{Z}, \end{array} \quad (\mathcal{G})$$

where Δx denotes the instantaneous change on the state x due to an impulse f_d. Now, consider the following assumption over the hybrid system $\mathcal{G}$.

Assumption 1 (Haddad et al. (2006)): assume $f_c(\cdot)$ is locally Lipschitz continuous on $\mathcal{D}$, $\mathcal{Z}$ is closed, and $f_d(x)\neq 0$ for $x\in\mathcal{Z}\backslash\partial\mathcal{Z}$. If $x\in\partial\mathcal{Z}$ is such that $f_d(x)=0$, then $f_c(x)=0$. If $x\in\mathcal{Z}$ is such that $f_d(x)\neq 0$, then $x+f_d(x)\notin\mathcal{Z}$.

If Assumption 1 holds, then the following theorem applies.

Theorem 1 (Haddad et al. (2006)): consider the system $\mathcal{G}$, assume $\mathcal{D}_c\subset\mathcal{D}$ is a compact positively invariant set with respect to $\mathcal{G}$, and assume that there exist a continuously differentiable function $V:\mathcal{D}_c\to\mathbb{R}$ such that

$$V'(x)f_c(x)\leq 0, \qquad x\in\mathcal{D}_c,\ x\notin\mathcal{Z}, \quad (49)$$

$$V(x+f_d(x))\leq V(x), \qquad x\in\mathcal{D}_c,\ x\in\mathcal{Z}. \quad (50)$$

Let $\mathcal{R}\triangleq\{x\in\mathcal{D}_c : x\notin\mathcal{Z}, V'(x)f_c(x)=0\}\cup\{x\in\mathcal{D}_c : x\in\mathcal{Z}, V(x+f_d(x))=V(x)\}$ and let $\mathcal{M}$ denote the largest invariant set contained in $\mathcal{R}$. If $x_0\in\mathcal{D}_c$, then $x(t)\to\mathcal{M}$ as $t\to\infty$.

Considering Assumption 1 and Theorem 1, let us prove this proposition.

Proposition 1: under the hypothesis of Assumption 1 and with the trigger law of Algorithm 1 active, consider $x\in\mathcal{M}$ with $\mathcal{M}$ an invariant set such that $\mathcal{M}\subset\mathcal{D}_c$ and $\partial\mathcal{M}\cap\partial\mathcal{D}_c=\emptyset$. Then, if $y_0=x+\delta x\notin\mathcal{M}$, $y(t)\to\mathcal{M}$ as $t\to\infty$.

Proof: since $\mathcal{M}\subset\mathcal{D}_c$ and $\partial\mathcal{M}\cap\partial\mathcal{D}_c=\emptyset$, as soon as $x+\delta x$ is outside $\mathcal{M}$, the trigger law activates and will command, through Algorithm 2, a single impulse steering back the state to the admissible set, $y\in S_D^p$, $S_D^p\subset\mathcal{M}$.

Regarding the problem considered in this paper, Assumption 1 holds since (7) is Lipschitz continuous for $e\in[0,1)$ and the trigger condition given by Algorithm 1 is based on a closed domain S_D^p. Moreover, Algorithm 2 guarantees that S_D^p is reachable.

Additionally, Proposition 1 implies a sufficient condition for the invariance of the set S_D^p, under application of the event-triggered controller, in the presence of continuous disturbances. Since S_D^p has been clearly defined in (15), Proposition 1 has to be studied by obtaining $\mathcal{D}_c$, which will be referred to as the invariant contracting set.

4.2 Out-of-plane invariance

Regarding the invariance of the out-plane admissible set $S_{D_y}^p$, the following continuously differentiable function is proposed

$$V_{y_m}=g_{y_m}=(d_4-ey_m)^2+d_5^2-y_m^2, \quad (51)$$

which is the same expression of the out-of-plane constraint described semi-algebraically in (18)-(19). Note that for both $\underline{y}$ and $\overline{y}$ constraints, Theorem 1 is fulfilled as

$$\frac{\partial V_{y_m}(D)}{\partial D}D'(\nu)=0, \qquad D\in\overline{\mathcal{D}}_{c,\text{out}}, D\in S_{D_y}^p, \quad (52)$$

$$V_{y_m}(D^+)\leq V_{y_m}(D), \quad D\in\overline{\mathcal{D}}_{c,\text{out}}, D\notin S_{D_y}^p, \quad (53)$$

where $\overline{\mathcal{D}}_{c,\text{out}}$ denotes the invariant set of states contained within the exterior boundary of $\mathcal{D}_{c,\text{out}}$. On the other hand, $\underline{\mathcal{D}}_{c,\text{out}}:=\{D\in\overline{\mathcal{D}}_{c,\text{out}},\ \text{s.t. } V_{y_m}(D^+)=V_{y_m}(D), D\notin S_{D_y}^p\}$ denotes the deadzone set. Hence, according to Theorem 1, the out-plane invariant set is the union of the out-plane admissible set and the deadzone set $\mathcal{M}_{\text{out}}=S_{D_y}^p\cup\underline{\mathcal{D}}_{c,\text{out}}$. Finally, note that Proposition 1 holds since $\mathcal{M}_{\text{out}}\subset\overline{\mathcal{D}}_{c,\text{out}}$ and $\partial\mathcal{M}_{\text{out}}\cap\partial\overline{\mathcal{D}}_{c,\text{out}}=\emptyset$ as it can be deduced from (47) which is the Minkowski sum of a convex bounded set with an ellipse having a hole on its interior. A computation of the previous sets for a case with $\underline{\Delta V}=\overline{\Delta V}$ is shown in Fig.1

4.3 In-plane invariance

To demonstrate the invariance of the in-plane admissible set the following functions are proposed

$$\begin{aligned} V_{x_m}&=\hat{g}_{x_m}=\sum_{i=0}^{4}\overline{\theta}_{x_m,i}(d_1,d_2)d_3^i,\\ V_{z_m}&=g_{z_m}=d_1^2+d_2^2-z_m^2, \end{aligned} \quad (54)$$

which are the same expressions as the in-track and radial constraints described semi-algebraically by (22)-(23) and (20)-(21). It can be easily shown that Theorem 1 is fulfilled by means of

$$\frac{\partial V_{w_{xz}}(D)}{\partial D}D'(\nu)=0,\ D\in\mathcal{D}_{c,\text{in}},\ D\in S_{D_{xz}}^p, \quad (55)$$

$$V_{w_{xz}}(D^+)\leq V(D),\ D\in\mathcal{D}_{c,\text{in}},\ D\notin S_{D_{xz}}^p, \quad (56)$$

where $w_{xz}=\{\underline{x},\overline{x},\underline{z},\overline{z}\}$. In view of (55)-(56), the in-plane invariant set is given by $\mathcal{M}_{\text{in}}:=S_{D_{xz}}^p$. Proposition 1 cannot be applied 1 until $\mathcal{D}_{c,\text{in}}$ is obtained for the considered scenario parameters. A set $\mathcal{D}_{c,\text{in}}$ computed numerically is shown in Fig.2 where, for the chosen parameters, Proposition 1 holds since $\mathcal{M}_{\text{in}}\subset\mathcal{D}_{c,\text{in}}$ and $\partial\mathcal{M}_{\text{in}}\cap\partial\mathcal{D}_{c,\text{in}}=\emptyset$.

5. SIMULATION RESULTS

To assess the performance of the proposed event-triggered predictive controller, a hovering phase scenario described in Table 1 is run. The simulation is done in MATLAB/Simulink using a non-linear relative motion simulator from Arantes Gilz (2016). Note that non-Keplerian forces are accounted for such as the $J2$ effect and atmospheric drag for both target and chaser vehicle.

Since the initial state is far from the admissible set, the 3-impulsive controller from Arantes Gilz et al. (2018) is used to reach S_D^p. Then, the local event-based controller

a = 8750 km, e=0.2, ν_0=0,
$\underline{\Delta V}$=1·10^{-3} m/s, $\overline{\Delta V}$=0.1 m/s
Initial relative position: [400, 300, -40] m
Initial relative velocity: [0, 0, 0] m/s
[$\underline{x}$, $\overline{x}$, $\underline{y}$, $\overline{y}$, $\underline{z}$, $\overline{z}$]=[50, 150, -25, 25, -25, 25] m

Table 1. Scenario parameters

takes the lead as soon as S_D^p is reachable. The controller threshold is δ=0.07 and the sampling sampling rate is such that the trigger rules of algorithm 1 are evaluated every 5° (in terms of true anomaly) along 10 target orbital periods.

As seen in Fig.3, the event-triggered predictive controller

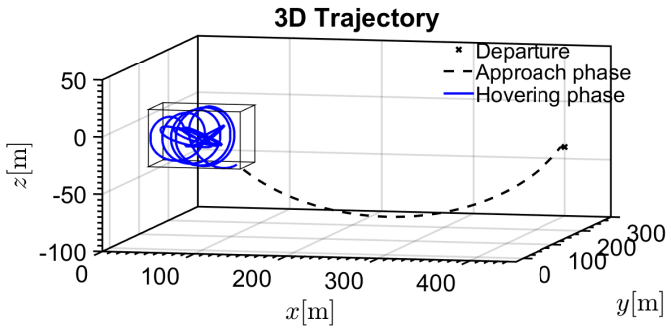

Fig. 3. Spacecraft trajectory.

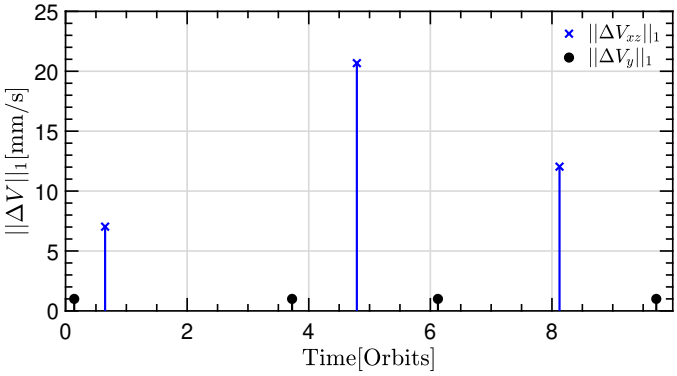

Fig. 4. Triggered impulses.

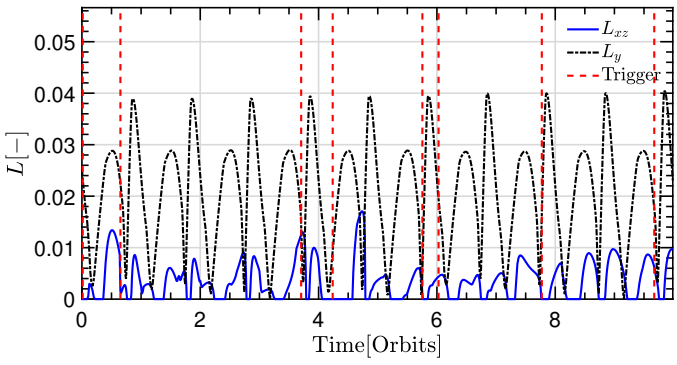

Fig. 5. Plot of L_{xz}, L_y and trigger signal.

achieves its purpose of maintaining the spacecraft at least close to the hovering zone. The commanded impulses are shown in Fig.4 where the limitation imposed by the deadzone condition can be observed on for the out-of-plane control. The oracle variables, L_{xz} and L_y and the

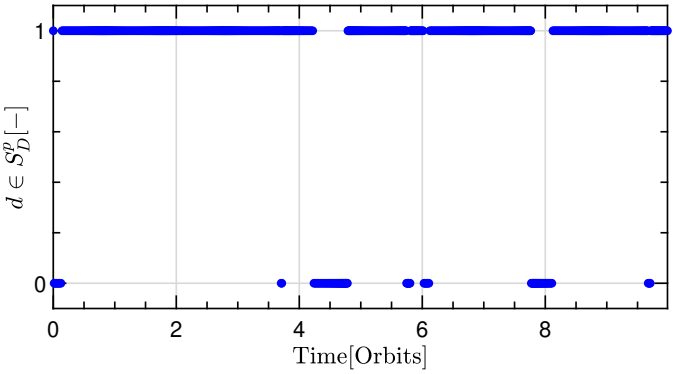

Fig. 6. Admissible set signal.

	J[cm/s]	N[-]	$X \in$ box[%]
Local	4.375	7	98.26
Global	6.336	15	94.44

Table 2. Comparison between local and global controllers.

trigger signal are shown in Fig.5 where it can be seen that 8 trigger signals are raised. Note that S_D^p is recovered after the trigger signal between orbits 5 and 6 is raised, see Fig.6, and hence only 7 impulses are necessary as seen in Fig.4.

Table 2 compares the local controller of this work with the global controller from Arantes Gilz et al. (2018). The comparison begins when the hovering zone is reached and is carried out over 10 orbits. The considered parameters for the global controller are τ_I=τ_E=5° and τ_S=60°. For the considered scenario, the event-triggered controller improves the performance criteria in terms of fuel consumption, J=$\sum_{i=1}^{N}\|\Delta V_i\|_1$, number of impulses N and the percentage $X \in$ box. The fuel consumption only accounts for applied impulses control. For instance, when the global controller computes impulses that fall within the deadzone, they are set to zero and are not considered in the cost J. The criterion "$X \in$ box" indicates the percentage of time that the chaser spacecraft lays inside the hovering box. Note that this criterion is different from the one shown in Fig. 6 because the condition $D \in S_D^p$ is sufficient for the chaser to lay inside the hovering zone.

6. CONCLUSIONS

In this paper, an event-triggered predictive controller is presented to locally maintain the spacecraft within the limits of the hovering zone, respecting both deadzone and saturation conditions. The control law is based on a single impulse driving the spacecraft back to the admissible set every time a trigger is raised. A study of invariance for the proposed approach has been made by using impulsive hybrid systems theory combined with reachability techniques. The main drawback of the proposed algorithm is that invariance for the in-plane motion has not been formally proven but only shown by numerical means for the scenario parameters. Future work may include a more formal analysis of the in-plane invariance and the possible consideration of multi-impulsive control laws to enlarge the reachable set.

REFERENCES

Arantes Gilz, P.R. (2016). A Matlab®/Simulink® non-linear simulator for orbital spacecraft rendezvous applications. URL `https://hal.archives-ouvertes.fr/hal-01413328`.

Arantes Gilz, P.R., Joldes, M., Louembet, C., and Camps, F. (2017). Model predictive control for rendezvous hovering phases based on a novel description of constrained trajectories. In *IFAC World Congress*, pp. 7490–7495. Toulouse, France.

Arantes Gilz, P.R., Joldes, M., Louembet, C., and Camps, F. (2018). Stable Model Predictive Strategy for Rendezvous Hovering Phases Allowing for Control Saturation. Submitted to *Journal of Guidance, Control and Dynamics*. URL `https://hal.archives-ouvertes.fr/hal-01678768`.

Aström, K.J. (2008). *Analysis and Design of Nonlinear Control Systems*, chapter Event Based Control, 127–147. Springer, Berlin, Heidelberg.

B. Reed, B., C. Smith, R., Naasz, B., F. Pellegrino, J., and E. Bacon, C. (2016). The Restore-L Servicing Mission. In *AIAA Space*.

Barnhart, D., Sullivan, B., Hunter, R., Bruhn, J., Fowler, E., M. Hoag, L., Chappie, S., Henshaw, G., E. Kelm, B., Kennedy, T., Mook, M., and Vincent, K. (2013). Phoenix Project Status - 2013. In *AIAA Space*.

Breger, L.S. and How, J.P. (2008). Safe Trajectories for Autonomous Rendezvous of Spacecraft. *Journal of Guidance, Control and Dynamics*, 31(5), 1478–1489.

Brentari, M., Urbina, S., Arzelier, D., Louembet, C., and Zaccarian, L. (2018). A Hybrid Control Framework for Impulsive Control of Satellite Rendezvous. *IEEE Transactions on Control Systems Technology*, 1–15.

Deaconu, G. (2013). *On the trajectory design, guidance and control for spacecraft rendezvous and proximity operations*. Ph.D. thesis, Univ. Toulouse 3 - Paul Sabatier, Toulouse, France.

Di Cairano, S., Park, H., and Kolmanovsky, I. (2012). Model Predictive Control approach for guidance of spacecraft rendezvous and proximity maneuvering. *International Journal of Robust and Nonlinear Control*, 22(12), 1398–1427.

Fix, G., Hsu, C.P., and Luo, T. (1996). Implicitization of Rational Parametric Surfaces. *Journal of Symbolic Computation*, 21(3), 329 – 336.

Gaias, G. and D'Amico, S. (2015). Impulsive Maneuvers for Formation Reconfiguration Using Relative Orbital Elements. *Journal of Guidance, Control and Dynamics*, 38(6), 1036 – 1049.

Haddad, W.M., Chellaboina, V., and Nersesov, S.G. (2006). *Impulsive and Hybrid Dynamical Systems*, chapter Stability Theory for Nonlinear Impulsive Dynamical Systems, 9–80. Princeton Series in Applied Mathematics.

Louembet, C. and Arantes Gilz, P.R. (2018). Event-triggered Model predictive control for spacecraft rendezvous. In *6th IFAC Conference on Nonlinear Model Predictive Control*. Madison, USA.

Pawlowski, A., Guzmán, J., Berenguel, M., and Dormido, S. (2015). *Event-Based Generalized Predictive Control*, 151–176.

Qi, R., Xu, S., and Xu, M. (2012). Impulsive Control for Formation Flight About Libration Points. *Journal of Guidance, Control and Dynamics*, 35(2), 484–496.

Tschauner, J. (1967). Elliptic Orbit Rendezvous. *AIAA Journal*, 5(6), 1110–1113.

Wu, B., Shen, Q., and Cao, X. (2018). Event-triggered attitude control of spacecraft. *Advances in Space Research*, 61, 927–934.

Wu, W., Reimann, S., and Liu, S. (2014). Event-Triggered Control for Linear Systems Subject to Actuator Saturation. In *19th IFAC World Congress*. Cape Town, South Africa.

Yamanaka, K. and Ankersen, F. (2002). New State Transition Matrix for Relative Motion on an Arbitrary Elliptical Orbit. *Journal of Guidance, Control, and Dynamics*, 25(1), 60–66.

Yang, X. and Cao, X. (2015). A new approach to autonomous rendezvous for spacecraft with limited impulsive thrust: Based on switching control strategy. *Aerospace Science and Technology*, 43, 454–462.

Zhang, C., Wang, J., Sun, R., Zhang, D., and Shao, X. (2018). Multi-spacecraft attitude cooperative control using model-based event-triggered methodology. *Advances in Space Research*, 62, 2620–2630.